Supporting Information

UV-Visible-Near-Infrared-Driven Photoelectrocatalytic Urea Oxidation and Photocatalytic Urea Fuel Cells Based on Ruddlensden–Popper-Type Perovskite Oxide La_2NiO_4

Mingwen Xiong [1,*,†], Ying Tao [2,†], Lanlan Fu [2], Donglai Pan [3], Yuxin Shi [2], Tong Hu [1], Jiayu Ma [1], Xiaofeng Chen [2,*] and Guisheng Li [2,3,*]

[1] School of Materials and Chemical Engineering, Bengbu University, Bengbu 233030, China
[2] School of Environmental and Geographical Sciences, Wetland Ecosystem Observation and Research Field Station, Shanghai Normal University, Shanghai 200234, China
[3] Key Laboratory of Resource Chemistry of Ministry of Education, Shanghai Normal University, Shanghai 200234, China
* Correspondence: xiongmingwen@163.com (M.X.); xiaofengchen@shnu.edu.cn (X.C.); liguisheng@shnu.edu.cn (G.L.)
† These authors contributed equally to this work.

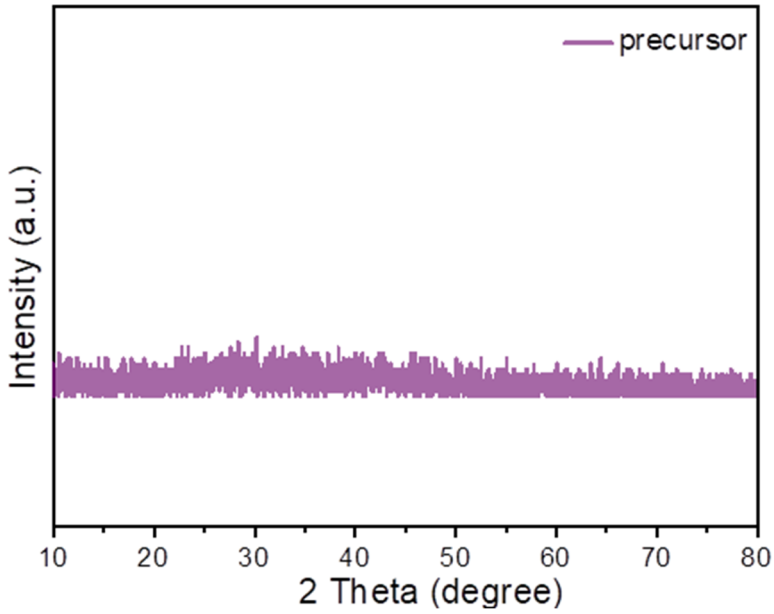

Figure S1. The XRD pattern of the La_2NiO_4 - precursor/rGO.

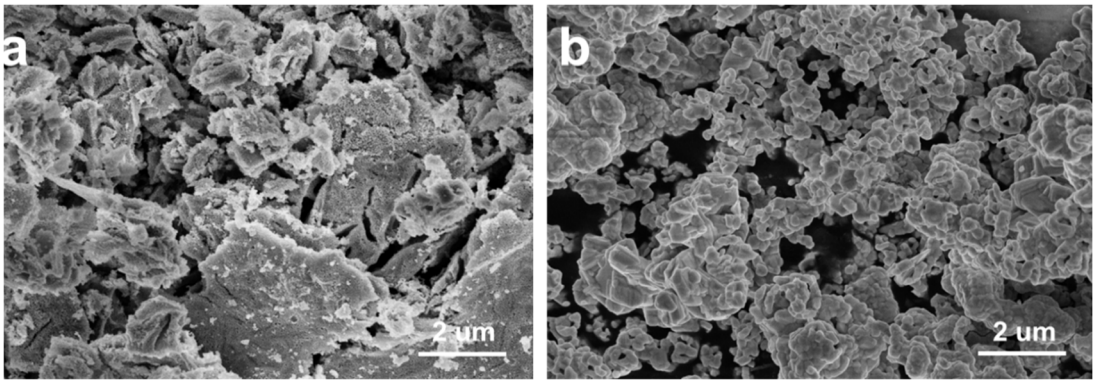

Figure S2. SEM of La_2NiO_4 with rGO (**a**) and without rGO (**b**).

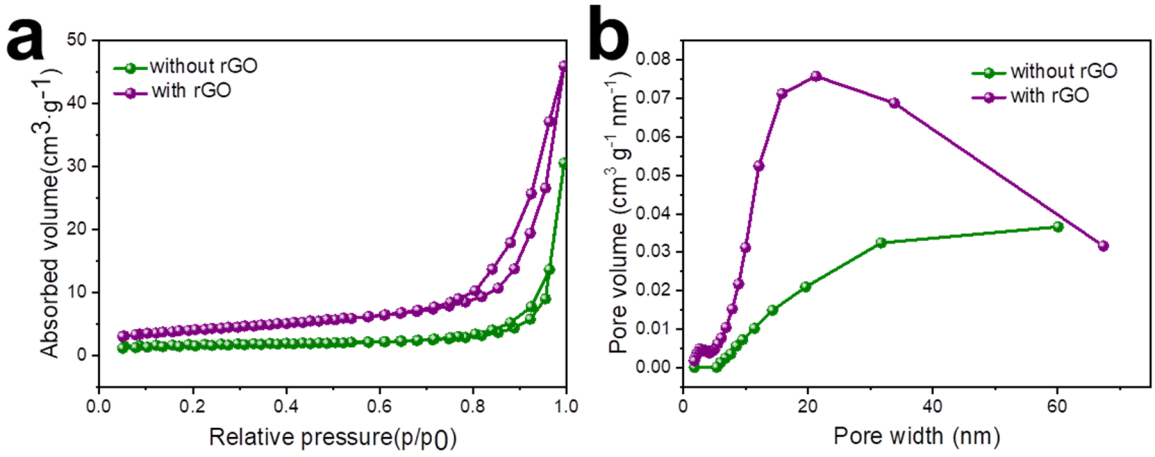

Figure S3. (**a**) Nitrogen adsorption-desorption isotherms and (**b**) Pore size distribution of La_2NiO_4 with and without rGO were added.

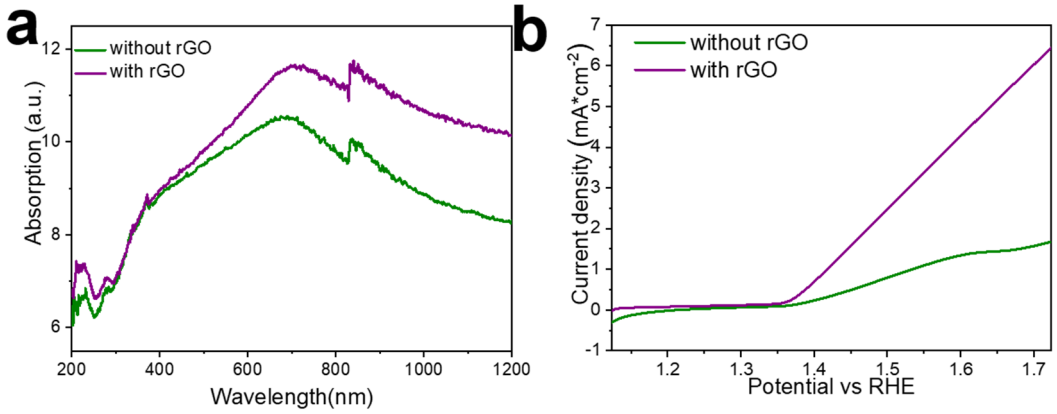

Figure S4. (**a**) The UV-vis-NIR diffuse reflectance spectra and (**b**) UOR activity under NIR light of La_2NiO_4 with and without rGO.

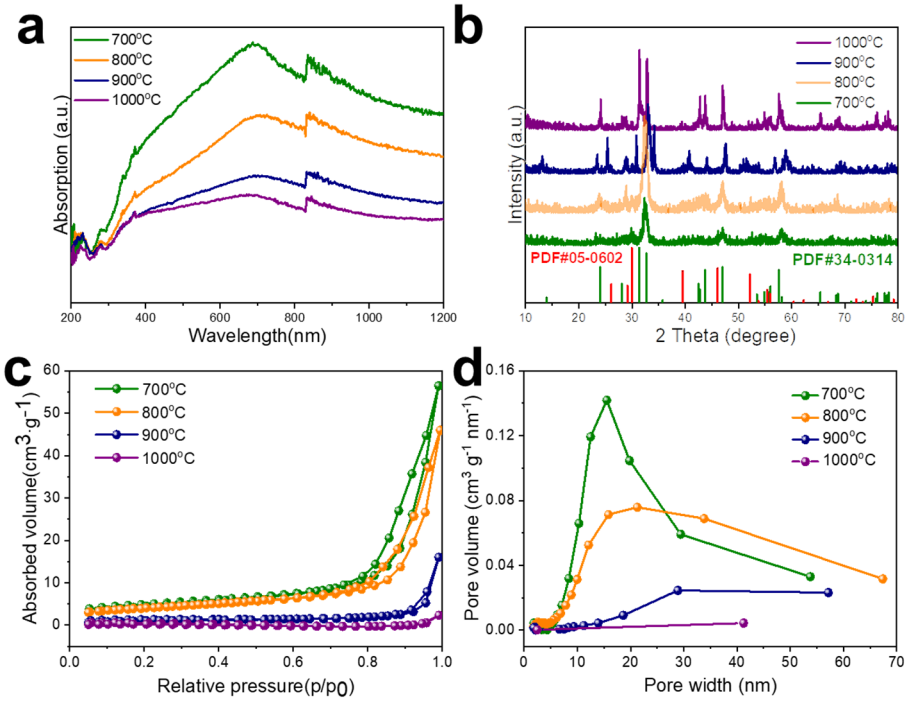

Figure S5. (**a**) The XRD pattern **(b)** The UV-vis-NIR diffuse reflectance spectra (**c**) Nitrogen adsorption-desorption isotherms and (**d**) Pore size distribution of La_2NiO_4 annealed at 700 °C, 800 °C, 900 °C and 1000 °C, respectively.

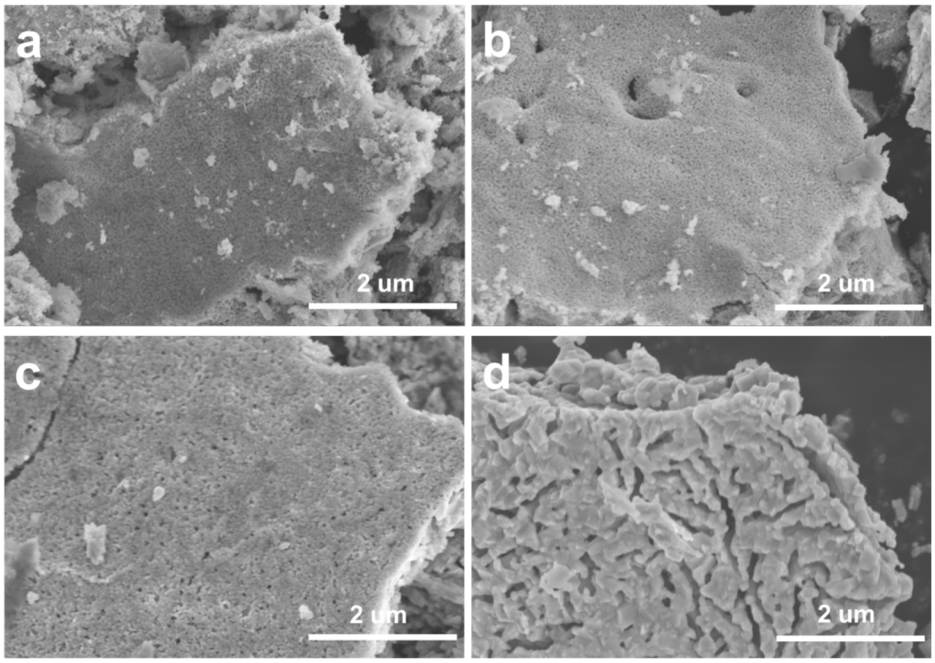

Figure S6. SEM images of La_2NiO_4 annealed at 700 ºC, 800 ºC, 900 ºC and 1000 ºC, respectively.

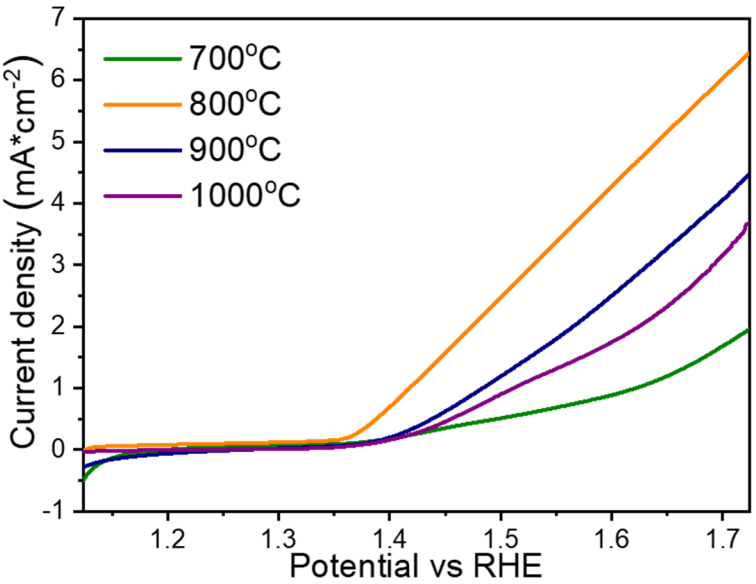

Figure S7. UOR activity under near-infrared light of La_2NiO_4 annealed at 700 ºC, 800 ºC, 900 ºC and 1000 ºC, respectively.

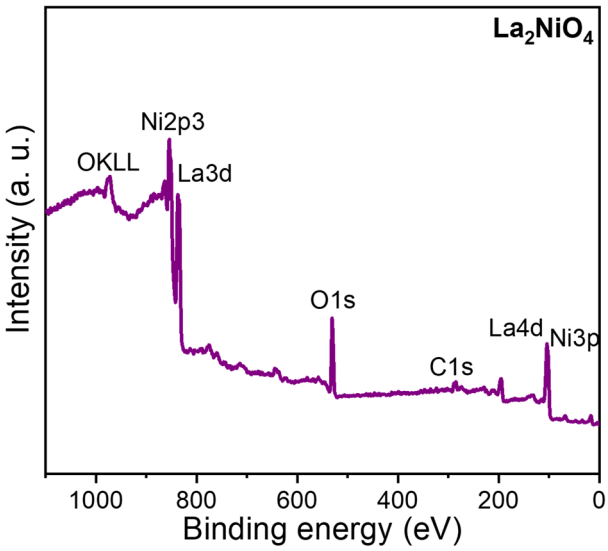

Figure S8. The XPS survey of La_2NiO_4.

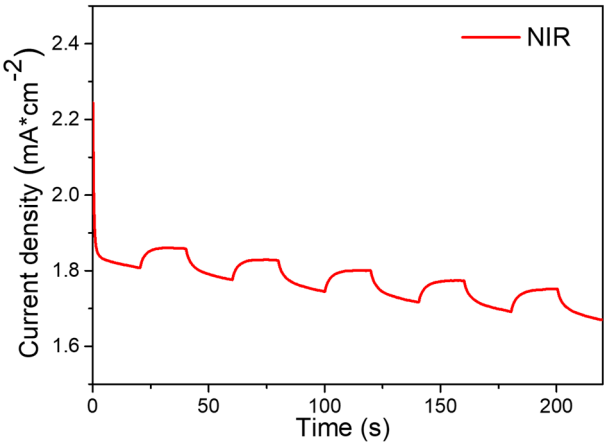

Figure S9. Photocurrent response of near-infrared light in 1 M KOH and 0.5 M urea electrolyte under low-power density light (100 mW cm^{-2}) and low temperature ice water bath.

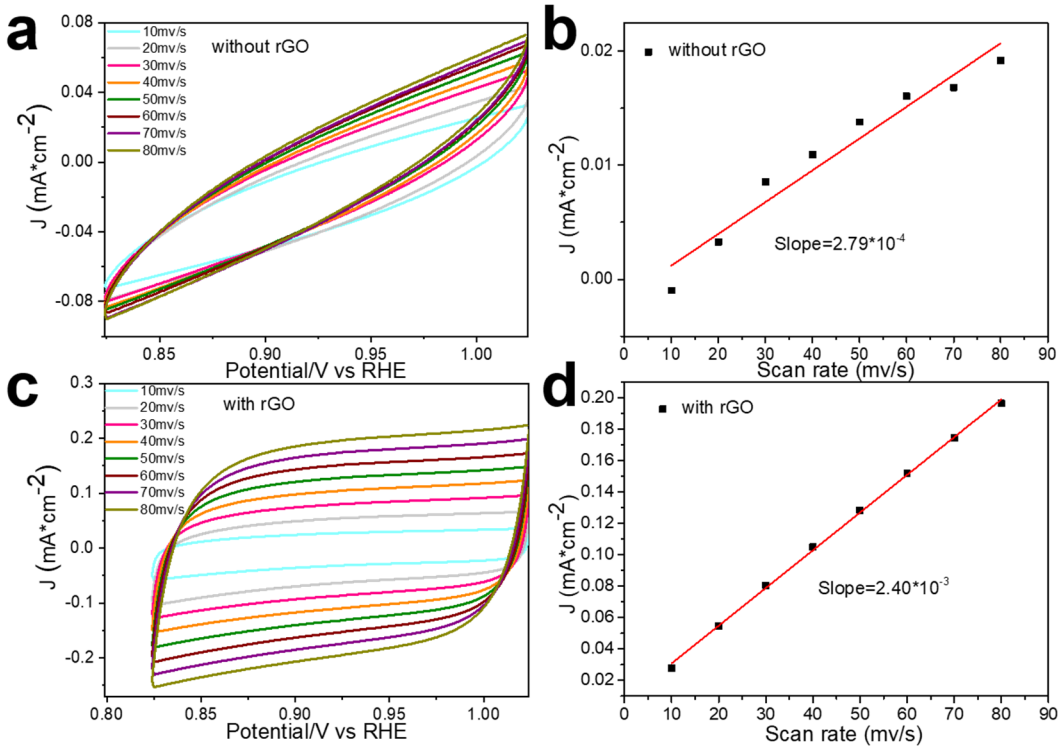

Figure S10. (**a**,**c**), Cyclic voltammetry for La_2NiO_4 with and without rGO in a non-Faradaic region of the potential range from 0.82~1.02 V vs. RHE at scan rate from 10 to 80 mV s^{-1} measured in 1.0 M KOH solution with 0.5 M urea. (**b**,**d**) The calculated Cdl. The current density at the potential of the 0.92 V vs. RHE ploted with the scan rates.

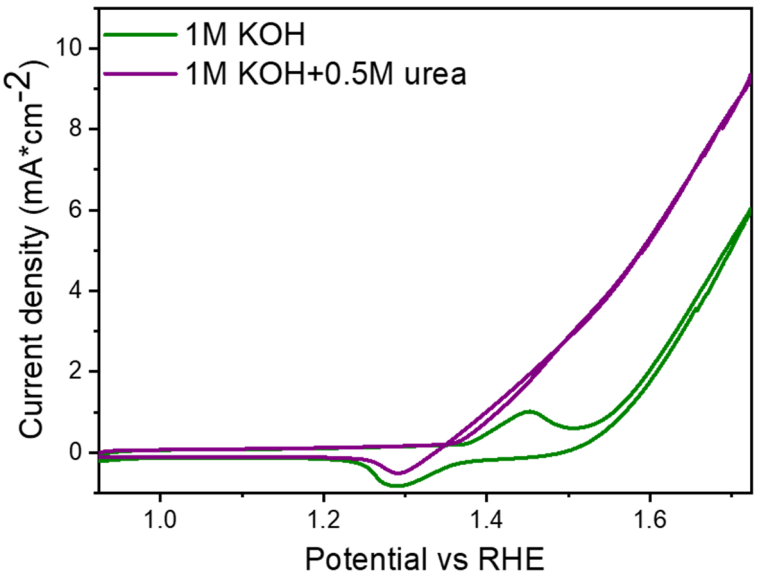

Figure S11. Cyclic voltammetry (CV) curves of La_2NiO_4 in 1 M KOH electrolyte with and without 0.5 M urea.

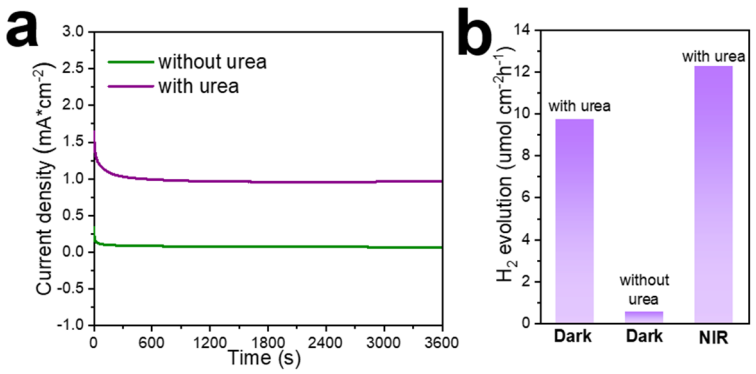

Figure S12. (**a**) Chronoamperometry responses (j–t) of the 1 M KOH and 1 M KOH with 0.5 M urea at applied potential of 1.47 V vs. RHE under dark. (**b**) Hydrogen production at applied potential of 1.47 V vs. RHE under different reaction conditions. All processes were performed without special instructions at a concentration of 1 M KOH with 0.5 M urea.

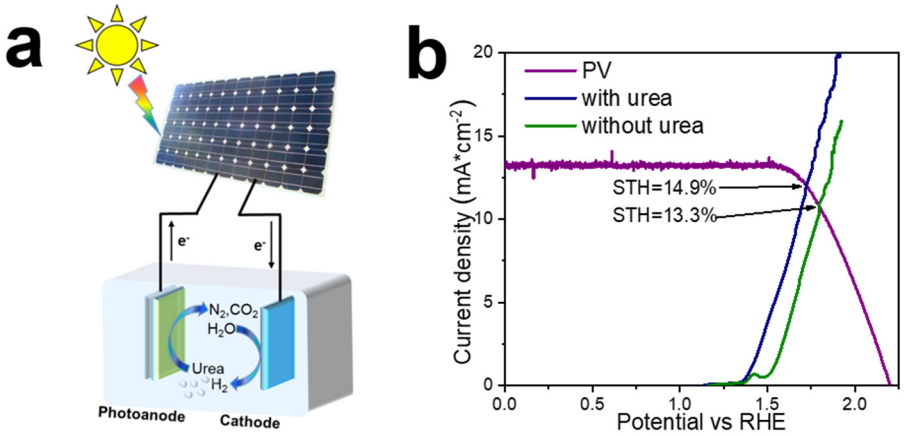

Figure S13. (**a**) A Schematic diagram showing a commercial silicon solar cell-driven electrolysis of 1 M KOH with 0.5 M urea under sunlight. (**b**) Photocurrent density–potential curve (J–V) of the 1 M KOH or 1 M KOH with 0.5 M urea under UV-visible light and a commercial silicon solar cell under simulated AM 1.5-G 100 mW cm^{-2} illumination.

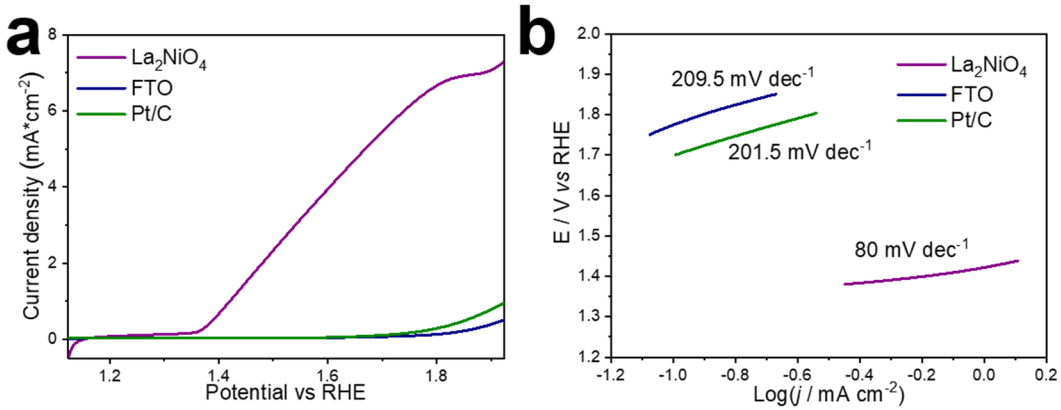

Figure S14. (**a**) UOR activity under dark of FTO, FTO coated with La_2NiO_4 and 5% Pt/C, respectively. (**b**) Tafel plots for the UOR derived from (**a**).

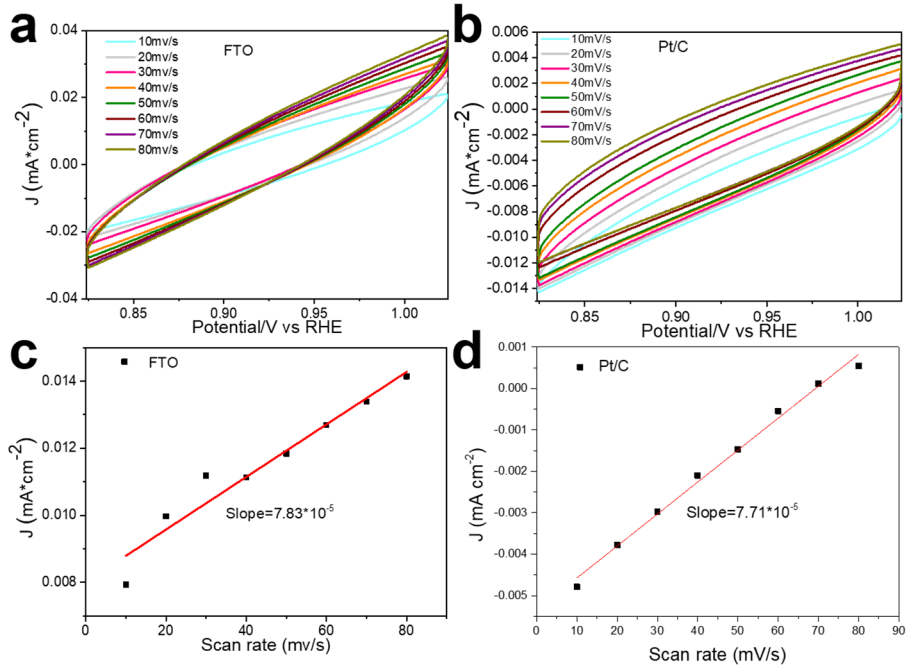

Figure S15. (**a**,**b**) Cyclic voltammetry for FTO and FTO coated with 5% Pt/C in a non-Faradaic region of the potential range from 0.82~1.02 V vs. RHE at scan rate from 10 to 80 mV s^{-1} measured in 1.0 M KOH solution with 0.5 M urea. (**c**,**d**) The calculated Cdl. The current density at the potential of the 0.92 V vs. RHE ploted with the scan rates.

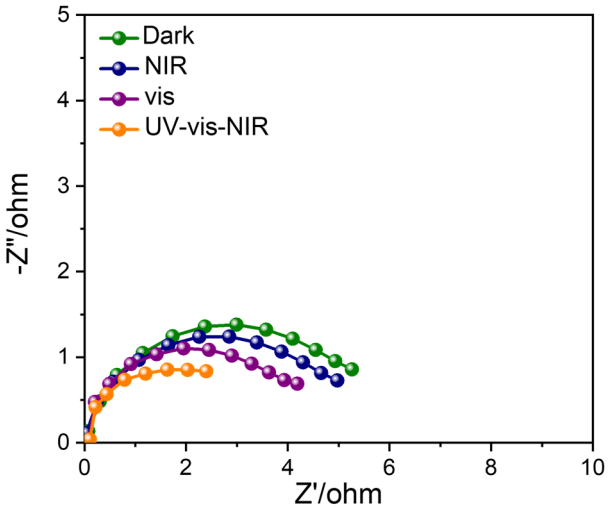

Figure S16. Nyquist plots of various light sources in urea solution at open circuit voltage vs. Hg/HgO.

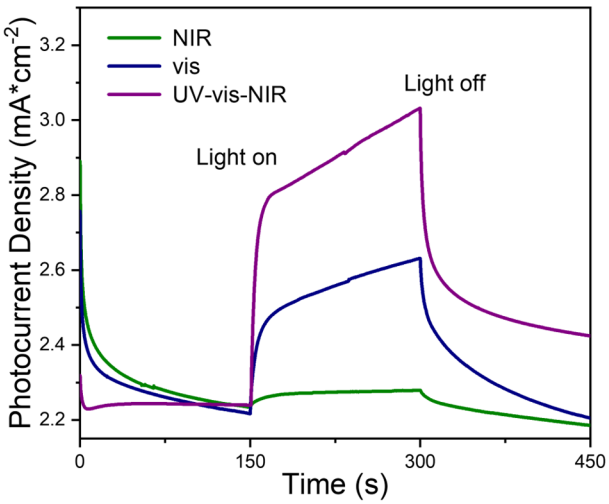

Figure S17. Photocurrent response of various light sources in urea solution.

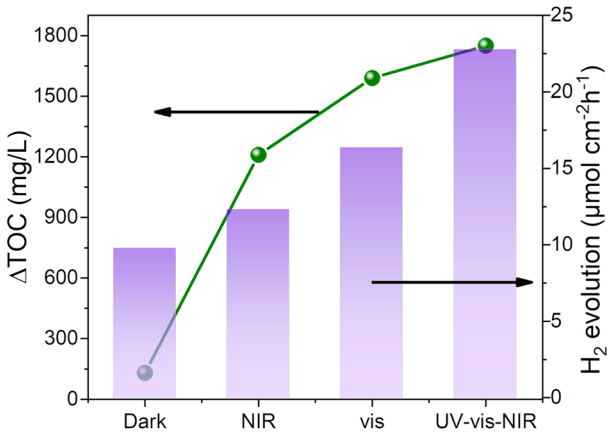

Figure S18. ΔTOC (urea) and Hydrogen production rates La_2NiO_4 for the UOR at

constant applied potentials of 1.47 V vs. RHE, respectively.

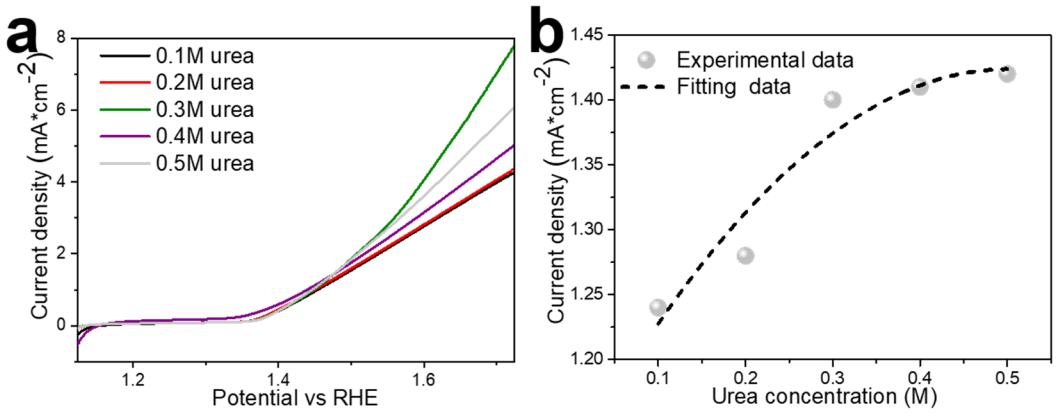

Figure S19. (**a**) Polarization curves for the UOR under urea concentration ranging from 0.1 to 0.5 M under NIR light irradiation. (**b**) The photocurrent density at a potential of 1.47 V vs. RHE derived from (**a**).

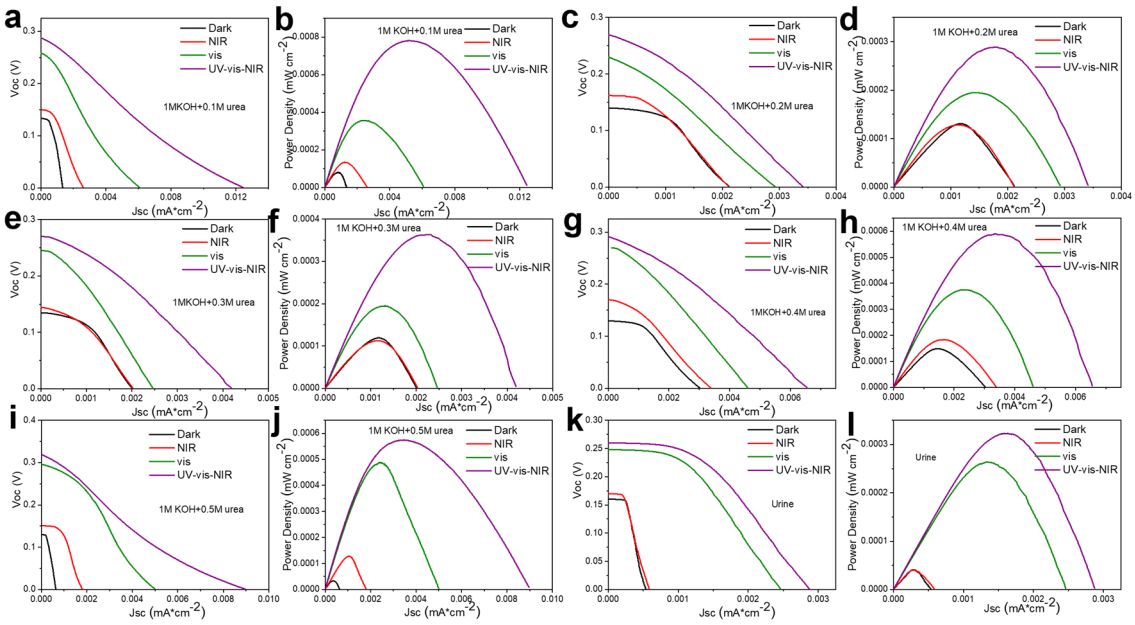

Figure S20. Polarization curves (*J-V* plots), and corresponding power density curves (*J-P* plots) of the PUFC device under urea concentration ranging from 0.1 to 0.5 M and human urine under various light sources irradiation.

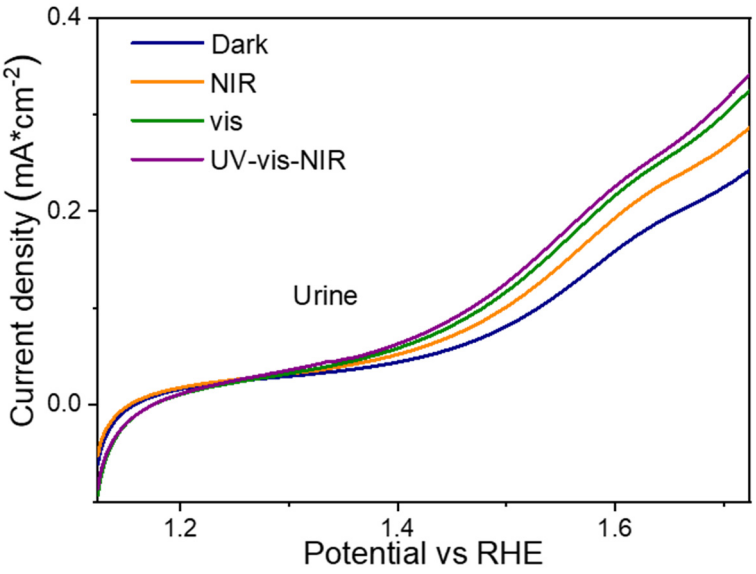

Figure S21. Polarization curves for the UOR under human urine.

Table S1. Performance parameters of PUFCs in 1 M KOH with 0.5 M urea exposed to different light sources irradiation.

Light source	Dark	NIR	vis	UV-vis-NIR
J_{sc} (μA cm^{-2})	0. 64	1.79	5.00	9.00
V_{oc} (V)	0.130	0.151	0.295	0.320
P_{max} (μW cm^{-2})	0.034	0.129	0.487	0.575
FF	0.409	0.477	0.330	0.200

The open-circuit voltage (VOC), short-circuit current density (JSC), and fill factor (FF) of the cell are listed in Table S1.The FF was calculated by the following equation, which could directly reflect the performance of the PUFC system:

$$FF = J*V_{max} /(J_{SC}*V_{OC})$$

where $J*V_{max}$ is the maximum power density of the PUFC obtained from the *J-P* plots. The fill factor respresents the deviation of the actual maximum power density produced by the cell from the value of $J_{sc}*V_{oc}$, which is the product of the highest possible values of current density and voltage. The performance of a fuel cell is directly related to its fill factor and should be optimized as much as possible.

Table S2. Performance parameters of PUFCs under urea concentration ranging from 0.1 to 0.5 M and human urine exposed to NIR light irradiation.

NIR	0.1 M urea	0.2 M urea	0.3 M urea	0.4 M urea	0.5 M urea	urine
J_{sc} (mA cm^{-2})	$2.61*10^{-3}$	$2.12*10^{-3}$	$2.02*10^{-}$	$3.37*10^{-3}$	$1.79*10^{-3}$	$5.9*10^{-4}$
V_{oc} (V)	0.149	0.162	0.145	0.170	0.151	0.169
P_{max} (mW cm^{-2})	$1.37*10^{-4}$	$1.29*10^{-4}$	$1.13*10^{-4}$	$1.85*10^{-4}$	$1.29*10^{-4}$	$4.1*10^{-5}$
FF	0.352	0.376	0.386	0.323	0.477	0.411